2.7 Turbines for hydroelectric power

[W. Braitsch, H. Haas]

2.7.1 Introduction

2.7.1.1 Theory of turbines

The first true high-efficiency water turbine was constructed by Benoit Fourneyron in 1824-27. Its first installation was in a saw-mill in Pont sur l'Ognon (France). Fourneyron's turbine was of the radial-outflow type (Fig. 2.7.1) and reached a maximum efficiency of 85%. An early Fourneyron turbine in St. Blasien (Germany), head 108 m, speed 2200 rpm, is known to have had a capacity of 25 kW with a runner diameter of only 312 mm – an incredible density of power at a time of water wheel drives.

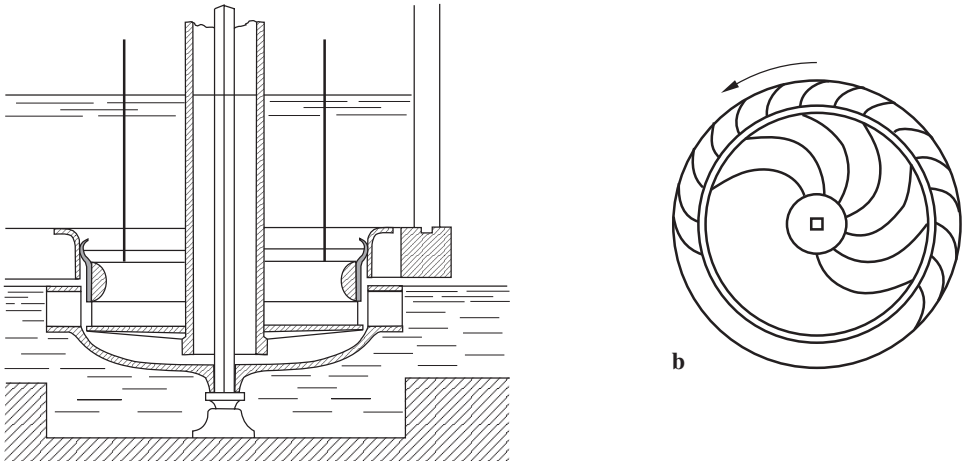

Fig. 2.7.1. Fourneyron turbine [97Koe]. **(a)** Meridional section. **(b)** Cross section.

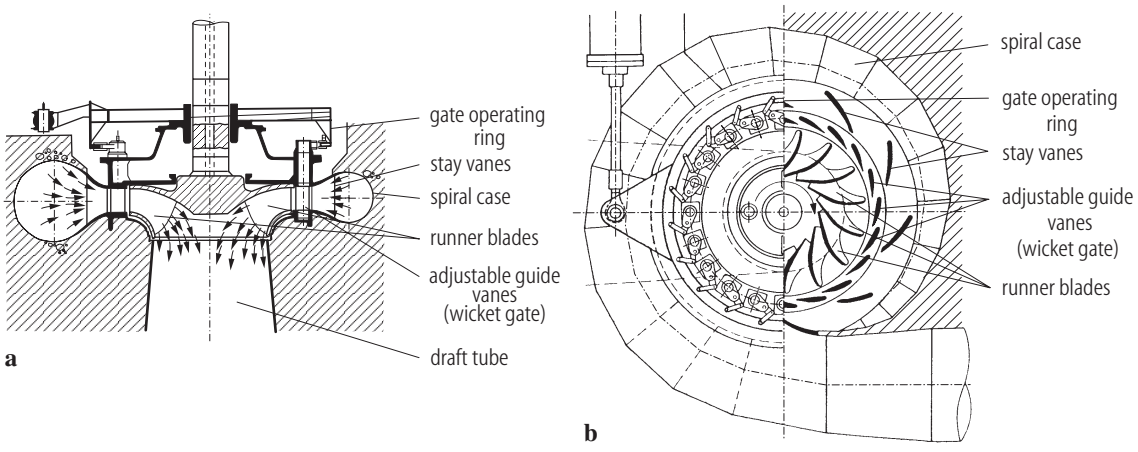

Fig. 2.7.2. Vertical Francis turbine. **(a)** Meridional section. **(b)** Cross section.

The reason for the superiority of a turbine is its sophisticated working principle. Conversion of flow energy to shaft power is based on the change of angular momentum of a continuous fluid flow in a runner. To illustrate this working principle, let us look at a water turbine of today, e. g. a Francis turbine (see Fig. 2.7.2). The Francis turbine is of the radial-inflow type. A spiral case, stay vanes and adjustable guide vanes cause the water to enter the runner with a distinct angular momentum in the direction of rotation. On the other hand, the curved runner blades force the water to leave the runner – at least at best efficiency point – with zero angular momentum. To understand this fact, consider the velocity triangles in Fig. 2.7.3. Note that the fluid velocity vector at a certain location within the runner may be described from an inertial frame of reference (absolute velocity vector $\boldsymbol{c}$) or from a frame of reference rotating with the runner (relative velocity vector $\boldsymbol{w}$). Kinematics shows that the absolute velocity vector $\boldsymbol{c}$ equals the vector sum $\boldsymbol{w} + \boldsymbol{u}$, where $\boldsymbol{u}$ is the (tangential) velocity vector of the rotating frame of reference at the respective location (so-called blade velocity). The graphical illustration of the vector relation $\boldsymbol{c} = \boldsymbol{w} + \boldsymbol{u}$ yields a velocity triangle.

In turbomachinery theory it is expedient to mark a location with a higher amount of energy also with a higher index. Hence we will denote the runner entrance of a turbine with index 2 and the runner exit with index 1. At the runner entrance (point 2, radius r_2, blade velocity vector $\boldsymbol{u_2}$) the absolute velocity vector $\boldsymbol{c_2}$ is given from upstream conditions (direction parallel to the guide vanes, norm resulting from continuity). $\boldsymbol{c_2}$ has a tangential component $\boldsymbol{c_{u2}}$ in the direction of the blade velocity $\boldsymbol{u_2}$. Note that the product $r_2 \cdot c_{u2}$ is the angular momentum per unit mass with respect to the turbine axis. Furthermore, $\boldsymbol{c_2}$ has a component $\boldsymbol{c_{m2}}$ perpendicular to the tangential direction, the so-called meridional component, which is proportional to the volume flow rate. The relative velocity vector $\boldsymbol{w_2}$ (viewed from the rotating runner) is equal to the vector difference $\boldsymbol{c_2} - \boldsymbol{u_2}$. Its direction at best efficiency point is parallel to the runner blades (shock-less entry). The curved runner blades now force the relative flow (and hence the relative velocity vector) to change its direction between entrance and exit.

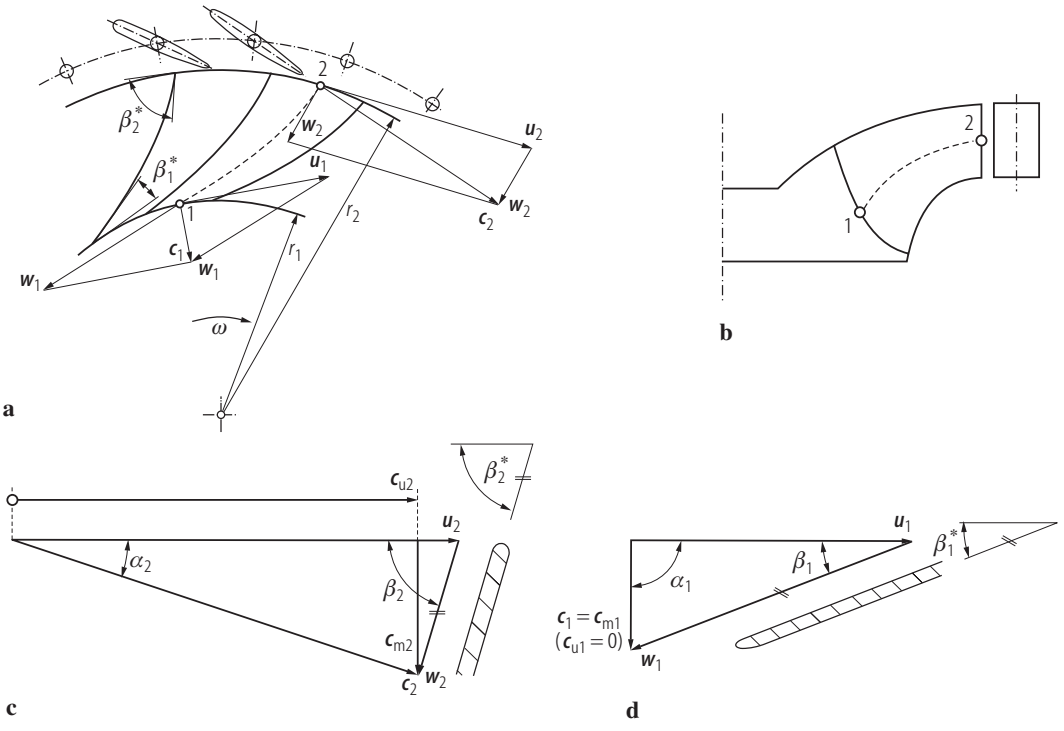

Fig. 2.7.3. (a) Velocity triangles of a Francis turbine at best efficiency point (simplified graphical representation of the blading as a plane radial cascade). β - angle of the flow; β^* - angle of the blade. **(b)** Meridional section of a Francis runner with runner entrance (point 2) and runner exit (point 1). **(c)** Velocity triangle at runner entrance (point 2). **(d)** Velocity triangle at runner exit (point 1).

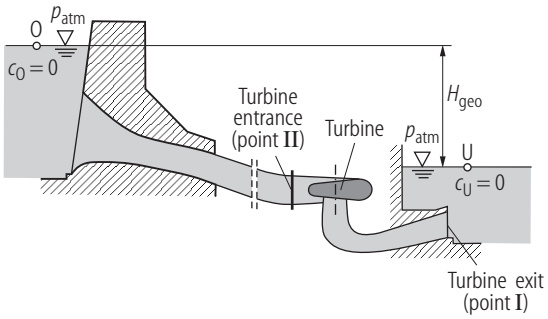

Fig. 2.7.4. Hydro power plant.

At the exit of the runner (point 1, radius r_1, blade velocity vector $\boldsymbol{u_1}$) the relative velocity vector $\boldsymbol{w_1}$ is given from upstream conditions (direction parallel to the runner blades, norm resulting from continuity). The absolute velocity vector $\boldsymbol{c_1}$ is equal to the vector sum $\boldsymbol{w_1} + \boldsymbol{u_1}$. $\boldsymbol{c_1}$ has a tangential component $\boldsymbol{c_{u1}}$, which at best efficiency point is equal to zero. Hence $r_1 \cdot c_{u1}$, the angular momentum per unit mass with respect to the turbine axis, is also equal to zero.

The change of angular momentum of the fluid between runner entrance and runner exit causes a torque T_B acting on the rotating blades. This torque is proportional to the angular momentum change per unit mass ($r_2 \cdot c_{u2} - r_1 \cdot c_{u1}$) and to the mass flow rate $\dot{m}_B$ passing through the runner blade row:

$$T_B = \dot{m}_B (r_2 c_{u2} - r_1 c_{u1}) \,. \tag{2.7.1}$$

Multiplying the torque T_B by the angular velocity ω of the rotating runner yields the power P_B delivered from the fluid to the blades (note that the product of angular velocity ω and radius r is equal to the respective blade velocity u):

$$P_B = T_B \omega = \dot{m}_B (u_2 c_{u2} - u_1 c_{u1}) \,. \tag{2.7.2}$$

Hence the power per mass flow rate (which is equivalent to the energy per unit mass, called specific blade energy w_B) reads

$$w_B = \frac{P_B}{\dot{m}_B} = u_2 c_{u2} - u_1 c_{u1} \,. \tag{2.7.3}$$

Equation (2.7.3) is the *Euler turbine equation*, derived by Leonhard Euler in 1754, some 70 years before the first useful turbine was constructed by Fourneyron.

Considering hydraulic applications, it is common practice to relate energies to the fluid weight instead of the fluid mass. The energies per unit weight have the evident dimension of a length (height). Let us hence introduce the specific blade energy per unit weight H_B, dividing w_B by the gravitational acceleration g:

$$H_B = \frac{w_B}{g} \,. \tag{2.7.4}$$

We now have to correlate the specific blade energy H_B to the specific fluid energy available at a hydro power plant (Fig. 2.7.4). The available energy per unit weight of an incompressible fluid (density ρ), entering the turbine at point II (pressure flange) and discharging at point I (draft tube exit), is the difference of the respective fluid-mechanical energies per fluid weight. This difference is called the head H of the turbine:

$$H = \left(\frac{p}{\rho g} + \frac{c^2}{2g} + z \right)_{II} - \left(\frac{p}{\rho g} + \frac{c^2}{2g} + z \right)_{I} \,. \tag{2.7.5}$$

Note that the fluid-mechanical energy consists of three terms, the pressure energy (displacement work) due to the pressure p, the kinetic energy due to the absolute velocity c and the potential energy due to the elevation z. Multiplying the head H (i.e. available energy per unit weight) by the weight flow rate $\dot{m}g$ passing through the turbine yields the total available power of the turbine, the so-called hydraulic power P_h:

$$P_h = \dot{m}gH \ . \tag{2.7.6}$$

An application of (2.7.5) to the whole hydro power plant (Fig. 2.7.4) between headwater (point O) and tailrace (point U) yields the gross available energy per unit weight to be equal to the geodetic head H_{geo} (same atmospheric pressure p_{atm} and zero velocities assumed at points O and U). An energy balance of the flow between headwater and tailrace shows that the head H defined in (2.7.5) is somewhat smaller than the geodetic head H_{geo} because of friction losses at intake, penstock and turbine exit (see also Sect. 2.1.2). Furthermore, an energy balance within the turbine shows that the specific blade energy H_B is smaller than the head H defined (2.7.5) because of flow friction losses within the turbine. The ratio H_B/H is called the hydraulic efficiency η_h of the turbine:

$$\eta_h = \frac{H_B}{H} \ . \tag{2.7.7}$$

Beside the flow friction losses there are further losses that reduce the net output available at the turbine shaft (volumetric losses due to the runner gaps, disc fiction losses, mechanical losses due to bearing and seal friction). The ratio of shaft power P_s to hydraulic power P_h is called the shaft efficiency η_s of the turbine:

$$\eta_s = \frac{P_s}{P_h} . \tag{2.7.8}$$

Additional losses occur in the turbine-driven generator (and in an eventual gear). The ratio of electric power P_{el} to hydraulic power P_h is called the overall efficiency η of the turbo set:

$$\eta = \frac{P_{el}}{P_h} . \tag{2.7.9}$$

2.7.1.2 Types of turbines

Since the days of Fourneyron many types of water turbines have been constructed. Most of them have vanished, among them Fourneyron's turbine (although we can still find turbines of the radial-outflow type in hydrodynamic transmissions). The evolution of nearly two centuries essentially left three types of water turbines that proved superior in a certain range of heads:

- Kaplan turbine (including the tubular turbine) for low heads;
- Francis turbine for medium heads;
- Pelton turbine for high heads.

Kaplan and Francis turbines are so-called reaction turbines, exhibiting a drop of static pressure in the runner between entrance and exit. Contrary, Pelton turbines are so-called action turbines with the same static pressure at runner entrance and exit. The application of the three main types of water turbines is illustrated in Fig. 2.7.5.

The abscissa of Fig. 2.7.5b needs an explanation: the quantity n_q, which systematically puts in order the different types of turbines, is a similarity parameter, the so-called specific speed. It is the speed in rpm of a geometric similar turbine with a volume flow rate Q of 1 m³/s and a head H of 1 m. From similarity

considerations based on Euler's equation (2.7.3) and continuity, n_q is calculated as

$$n_q = \frac{n\sqrt{Q}}{H^{3/4}}, \tag{2.7.10}$$

where n means the speed in rpm, Q the volume flow rate in m³/s and H the head in m. The specific speed n_q is a characteristic parameter for a certain type of turbine. It partly explains the application range of the different turbines: rearranging (2.7.10) yields the following expression for the speed n:

$$n = \frac{n_q H^{3/4}}{\sqrt{Q}}. \tag{2.7.11}$$

Hence the speed n is proportional to n_q and $H^{3/4}$, and inversely proportional to $Q^{1/2}$. A Pelton turbine, for example, with a very low specific speed n_q can only be applied at high heads and small volume flow rates in order to obtain an appropriate high shaft speed n.

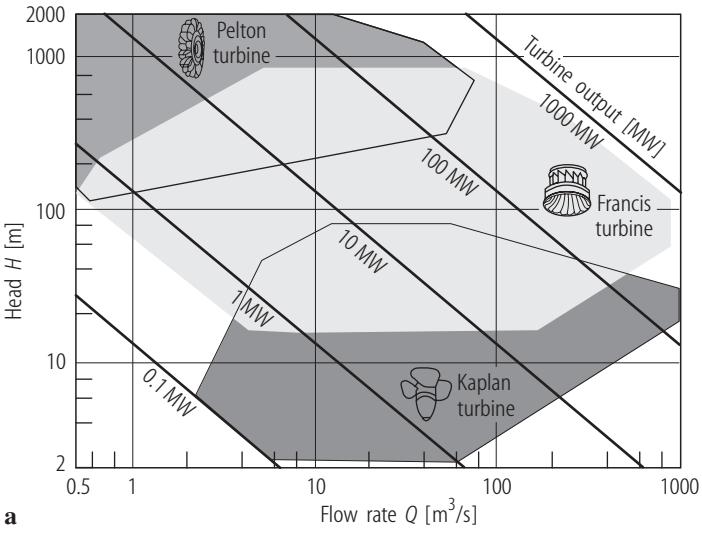

a

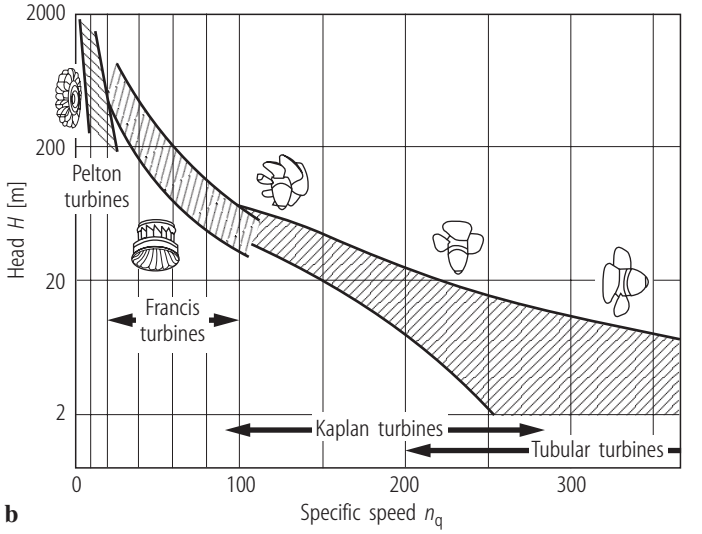

b

Fig. 2.7.5. Application of turbines. **(a)** Head H vs. flow rate Q [VAT]. **(b)** Head H vs. specific speed n_q [VSH].

Another important characteristic parameter that explains the application range of Kaplan and Francis turbines is the critical cavitation number $\sigma_{T,C}$, mentioned already in Sect. 2.2.4.3. Rearranging its defining equation yields the following expression for the suction head h_S (= z) in the critical case:

$$h_S = H_a - H_v - \sigma_{T,C} H \ . \tag{2.7.12}$$

Hence, assuming the cavitation number to be given for a certain type of turbine, the suction head h_S required for an operation without cavitation decreases with increasing head H. Furthermore, it is obvious from Fig. 2.2.15 that $\sigma_{T,C}$ increases with increasing specific speed n_q. Take as an example a Kaplan turbine with n_q = 250, $\sigma_{T,C}$ = 1.2 and a hypothetical head of H = 100 m. The atmospheric pressure head H_a amounts to about 10 m, the vapor pressure head H_v of cold water to about zero. Inserting these figures into (2.7.12), we obtain a suction head h_S = -110 m in the critical case. This means an arrangement of the turbine at least 110 m below the tailrace level which is usually not feasible. Thus, for a head of 100 m a turbine with lower specific speed and smaller critical cavitation number, namely a Francis turbine, is the appropriate solution.

Beside the three mentioned main types of turbines, some other types are customary, especially for small hydro power plants. A type of turbine frequently found in small plants is e.g. the Michell-Bánki turbine.

2.7.2 Francis turbines

The Francis turbine is based on a patent of Samuel Howd (1836). It is of the radial-inflow type and applied to medium heads up to 744 m (Häusling, Austria). The Francis turbine is the work-horse among the water turbines, producing the majority of hydro-electric energy in the world. At present, its output can amount up to 837 MW (Grand Coulee III, USA).

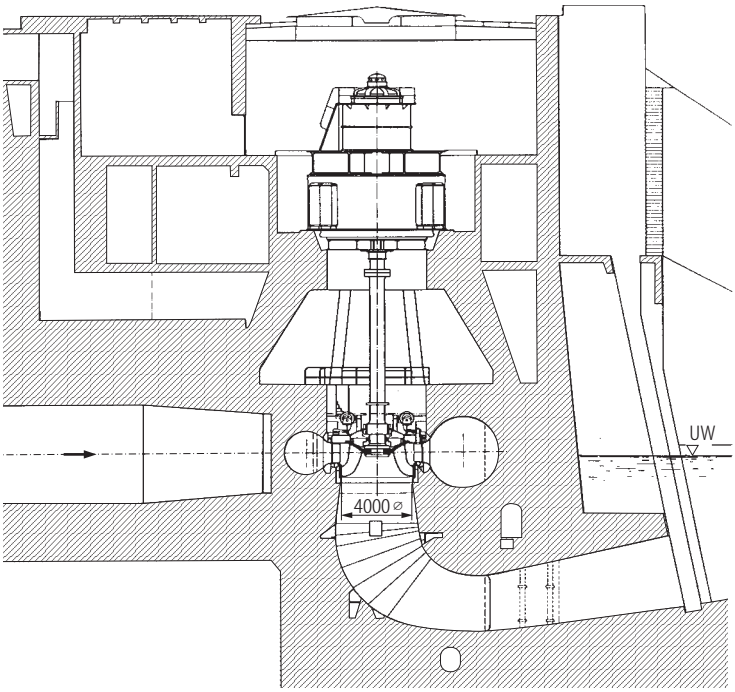

Fig. 2.7.6. Section of the Saucelle power plant (Spain) [VSH].

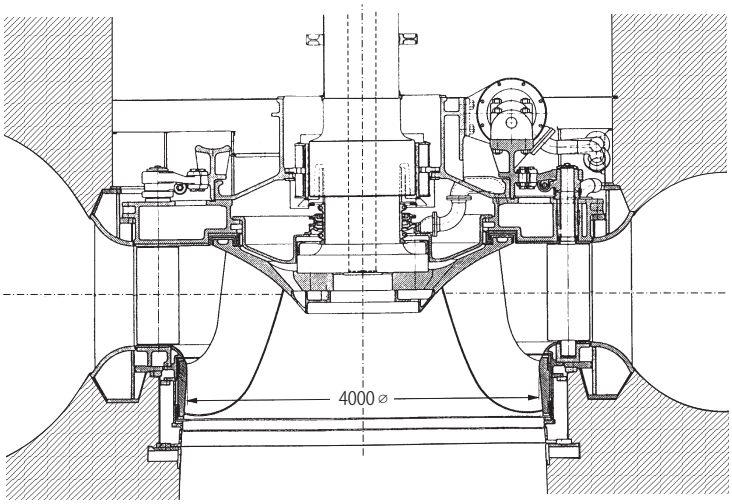

Fig. 2.7.7. Francis turbine of the Saucelle power plant (Spain) [VSH].

2.7.2.1 Example and working principle of a Francis turbine

Figure 2.7.6 shows a section of the Saucelle power plant (Spain), and Fig. 2.7.7 shows the section of one of the 4 turbines. The main data of this turbine are:

- Head: 62 m;
- Flow rate: 117 m^3/s;
- Speed: 150 rpm;
- Shaft power: 64 MW;

The working principle of a Francis turbine was already explained in Sect. 2.7.1.1. Regarding the Saucelle power plant, the water is supplied to each turbine via a penstock with a diameter of 5.7 m. A spiral case, stay vanes and 24 adjustable guide vanes cause the water to enter the runner with an angular momentum. Within the runner, equipped with 15 blades, the water's angular momentum decreases (At best efficiency point the angular momentum at the runner exit is equal to zero.) Besides, within the runner the water is deflected towards the axial direction and enters the draft tube (diffuser). Here the fluid is decelerated, discharging from the draft tube with a velocity c_1 that is as small as possible. Note that the kinetic energy of the fluid at the draft tube exit is lost. This is one of the flow losses reducing the gross available head H_{geo} of a hydro power plant (see Sect. 2.7.1.1).

The flow rate of the turbine (and hence the output) is controlled by the 24 adjustable guide vanes. The vanes are moved by a gate operating ring actuated by a hydraulic servo motor. The gate operating ring is linked to the vane levers, thus synchronously turning the guide vanes when moving. (see also Fig. 2.7.2). The turbine is directly coupled to the generator, as is usual in case of higher capacities.

2.7.2.2 Hydraulic design of a Francis runner

Figure 2.7.8 gives an impression of the design of a large Francis runner. The runner blades are usually profiled. The meridional shape of a Francis runner varies considerably dependent on specific speed n_q and head H (Fig. 2.7.9). The entrance-to-exit diameter ratio increases with increasing head. This ultimately is a consequence of Euler's equation (2.7.3): consider a Francis turbine with a given speed n at different heads. Assuming similar velocity triangles, a higher head requires a higher blade velocity at the runner entrance and hence a greater entrance diameter.

Fig. 2.7.8. Francis runner with a diameter of 6.14 m (Estreito, Brazil, P_{max} = 260 MW) [VSH].

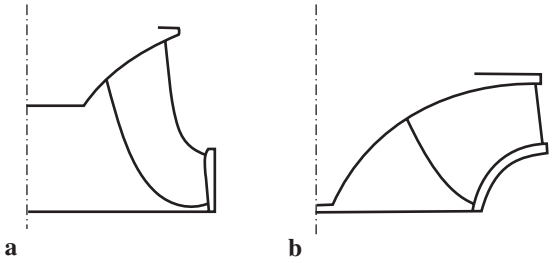

Fig. 2.7.9. Meridional shape of Francis runners of different specific speeds and heads.
(a) n_q = 73, H = 62 m (Saucelle, Spain).
(b) n_q = 31, H = 186 m (Reisach, Germany).

2.7.2.3 Manufacture of a Francis runner

A Francis runner may be manufactured by integral casting of the entire runner. However, more frequently it is manufactured by welding the individual components (crown, band, blades). A high-grade material for Francis runners is a stainless steel with 13% Cr (e.g. the ferritic steel G-X5CrNi13.4, material number 1.4313 according to DIN-EN 10020). A cheaper method is to use low-grade cast steel as base material and to coat critical areas with a welded overlay from stainless steel. The profiled shape of the steel-cast blades is obtained by milling, sometimes also by pressing after having milled the profile in the flat state from a plane steel sheet.

2.7.2.4 Operating problems with Francis turbines

Francis turbines are frequently subject to vibrational problems. In most cases the cause of the trouble is a swirl of water in the draft tube at off-design conditions. The reason of this swirl will be described in more detail in Sect. 2.7.6.1. The vibrational problems may be cured e.g. by special inserts in the draft tube or by air injection.

Abrasive water is another source of trouble, causing rapid wear of the runner gap seals. A remedy that is nowadays applied is an abrasion resistant coating with a hard material phase from tungsten carbide, thermally sprayed upon the gap surfaces.

2.7.2.5 Pump turbines

In pumped storage plants Francis-type pump turbines are frequently installed instead of separate pumps and turbines. As an example, Fig. 2.7.10 shows one of the pump turbines Langenprozelten (Germany). Although the meridional section of a pump turbine generally looks quite similar to that of a Francis turbine with low specific speed, there is a distinct difference in the shape of the runner blades (Fig. 2.7.11). In principle, pump turbines are centrifugal pumps with few backward-swept blades. Centrifugal pumps can work as turbines as well, but their turbine efficiency is lower than the efficiency of a Francis turbine which usually has a comparatively high number of forward-swept blades. The reason for the different blade geometry of a centrifugal pump is the completely different behavior of the boundary layer in a flow against a pressure increase as compared to a flow along with a pressure drop. As first recognized by Ludwig Prandtl in 1904, a pressure increase in the flow direction may possibly cause the boundary layer to separate, with detrimental effects on performance in case of a pump. Experience shows that boundary layer separation does not occur when the pressure rises only smoothly in the flow direction. Hence centrifugal pumps are usually equipped with backward-swept blades, resulting in a smooth rise of angular momentum and pressure within the blade row.

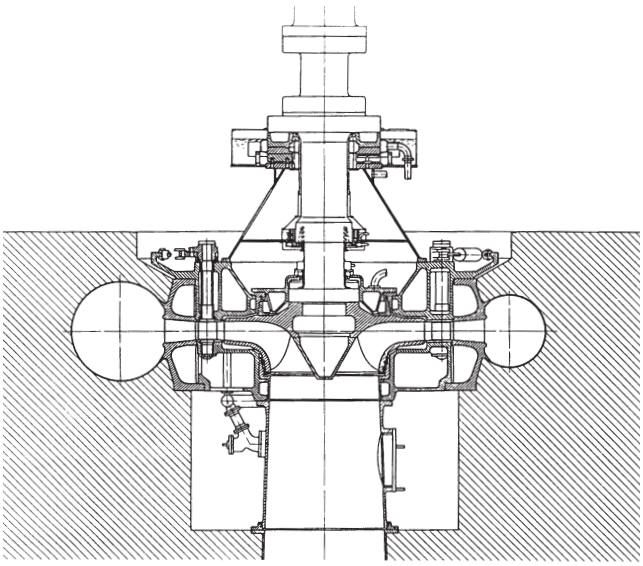

Fig. 2.7.10. Pump turbine Langenprozelten (Germany) with H = 278.6-305.5 m, P_S = 73.5-78.0 MW (turbine operation).

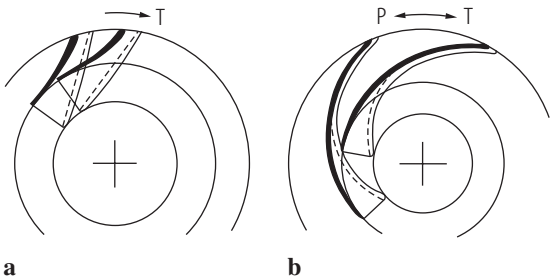

Fig. 2.7.11. Shape of runner blades. P stands for pumping, T for turbining operation [89Raa]. **(a)** Francis turbine. **(b)** Pump turbine.

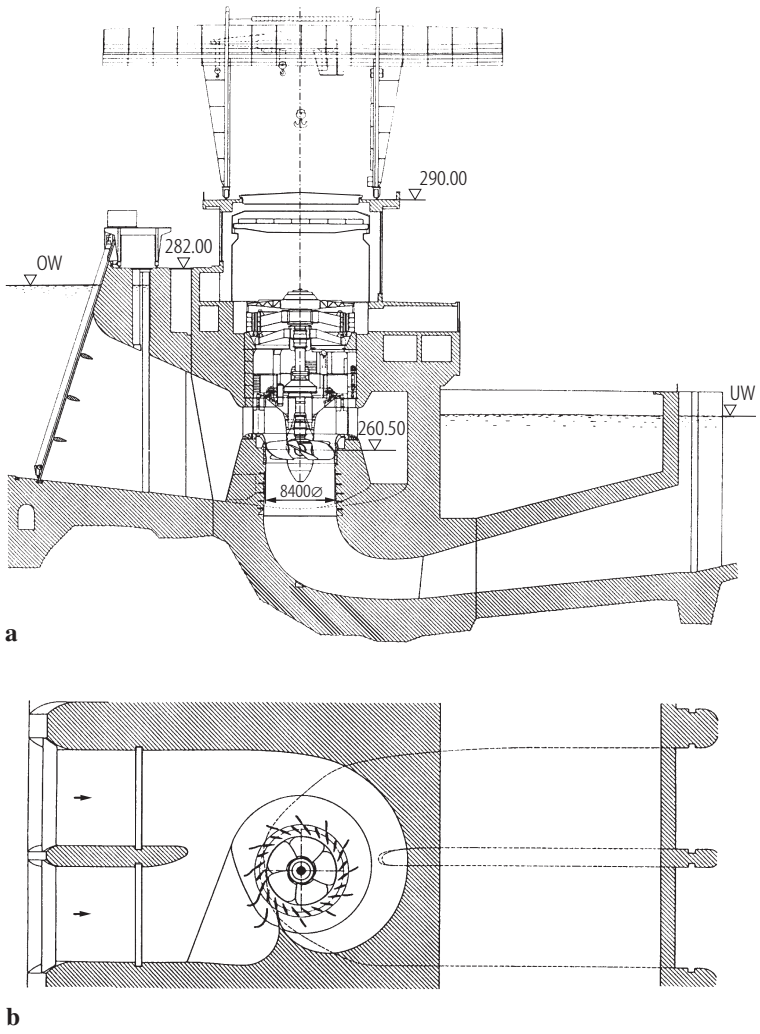

Fig. 2.7.12. Section of the Aschach power plant (Austria) [VSH]. **(a)** Longitudinal section. **(b)** Cross section.

2.7.3 Kaplan turbines

The Kaplan turbine was invented by Viktor Kaplan in 1912. It is of the axial-flow type and applied to low heads up to about 75 m (St. Martin, Austria). It is the typical turbine of low-head run-of-river plants. The most powerful Kaplan turbines today are installed in the Iron Gate power plant (Romania/Serbia), with an output of 200 MW each.

2.7.3.1 Example and working principle of a Kaplan turbine

As an example, Fig. 2.7.12 shows a section of the Aschach power plant in Austria; Fig. 2.7.13 shows a section of one of its turbines which have the following main data:

- Head: 15 m;
- Flow rate: 500 m^3/s;
- Speed: 68.2 rpm;
- Shaft power: 75 MW.

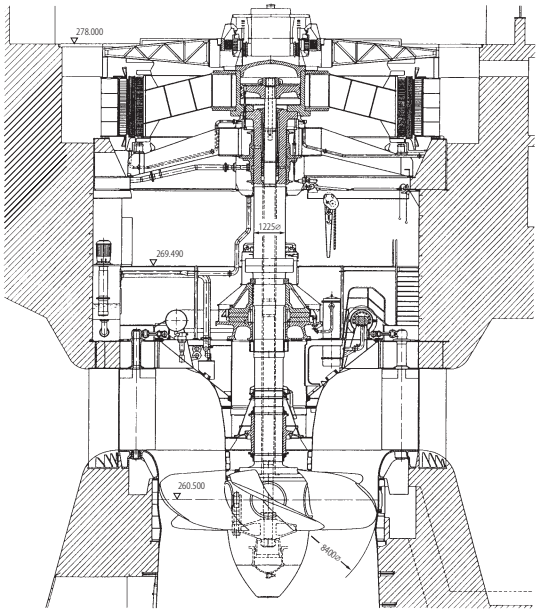

Fig. 2.7.13. Section of a Kaplan turbine of the Aschach power plant (Austria) [VSH].

The working principle of a Kaplan turbine does not differ much from that of a Francis turbine. Again a spiral case, stay vanes and adjustable guide vanes cause an angular momentum of the fluid. But contrary to the Francis turbine, the swirling fluid is deflected towards the axial direction before it enters the runner that resembles a ship propeller. Within the runner the water's angular momentum decreases and it leaves the runner – at least at best efficiency point – with zero angular momentum. This is readily understood considering the velocity triangles in Fig. 2.7.14. Basically, the description already given for the Francis turbine in Sect. 2.7.1.1 (Fig. 2.7.3) is also valid for the Kaplan turbine. In Fig. 2.7.14b/c the triangles are drawn for the tip section (Index a, blade velocity $\boldsymbol{u}_a$) and the hub section (Index i, blade velocity $\boldsymbol{u}_i$). Two additional remarks will help to understand the design of these triangles:

- The guide vanes, the axes of which are arranged on a cylindrical surface, generate a constant angular momentum per unit mass $r \cdot c_u$ for each fluid particle. In the transition duct between guide vanes and runner, the angular momentum is conserved. Hence a fluid particle entering the runner at the tip (radius r_a) has a smaller tangential component c_{u2a} than a fluid particle entering the runner at the hub (radius $r_i < r_a$), the latter exhibiting the tangential component $c_{u2i} > c_{u2a}$.
- The meridional velocity component c_m is constant within the runner. This is not an arbitrary assumption, but can be proved by a more detailed flow analysis based on the differential equation of motion.

From the velocity triangles the relative velocity vectors $\boldsymbol{w}$ are known. The essential task of the curved runner blades is to force the relative velocity to change its direction between entrance and exit of the runner. Hence a blade shape as drawn in Fig. 2.7.14d is necessary. Leaving the runner, the fluid enters the draft tube (diffuser), just as it is the case in a Francis turbine. In the draft tube the water is decelerated in order to obtain an exit velocity that is as small as possible.

The turbine is directly coupled to the generator. As with the Francis turbine, the flow rate (and hence the output) of the Kaplan turbine is controlled by the adjustable guide vanes. But contrary to the Francis turbine the Kaplan turbine has an essential additional feature: adjustable runner blades. This has a beneficial effect upon part load efficiency, as will be explained in greater detail in Sect. 2.7.6.2. The runner blades are moved by a rotating hydraulic servo motor which, in case of the Aschach turbine (Fig. 2.7.13), is situated in the generator hub. The mechanical arrangement for the runner vane adjustment is illustrated in Fig. 2.7.15. The rotating servo motor axially moves a crosshead in the runner hub via a rod. The crosshead is linked to the blade levers, thus synchronously turning the blades when moving in axial direction.

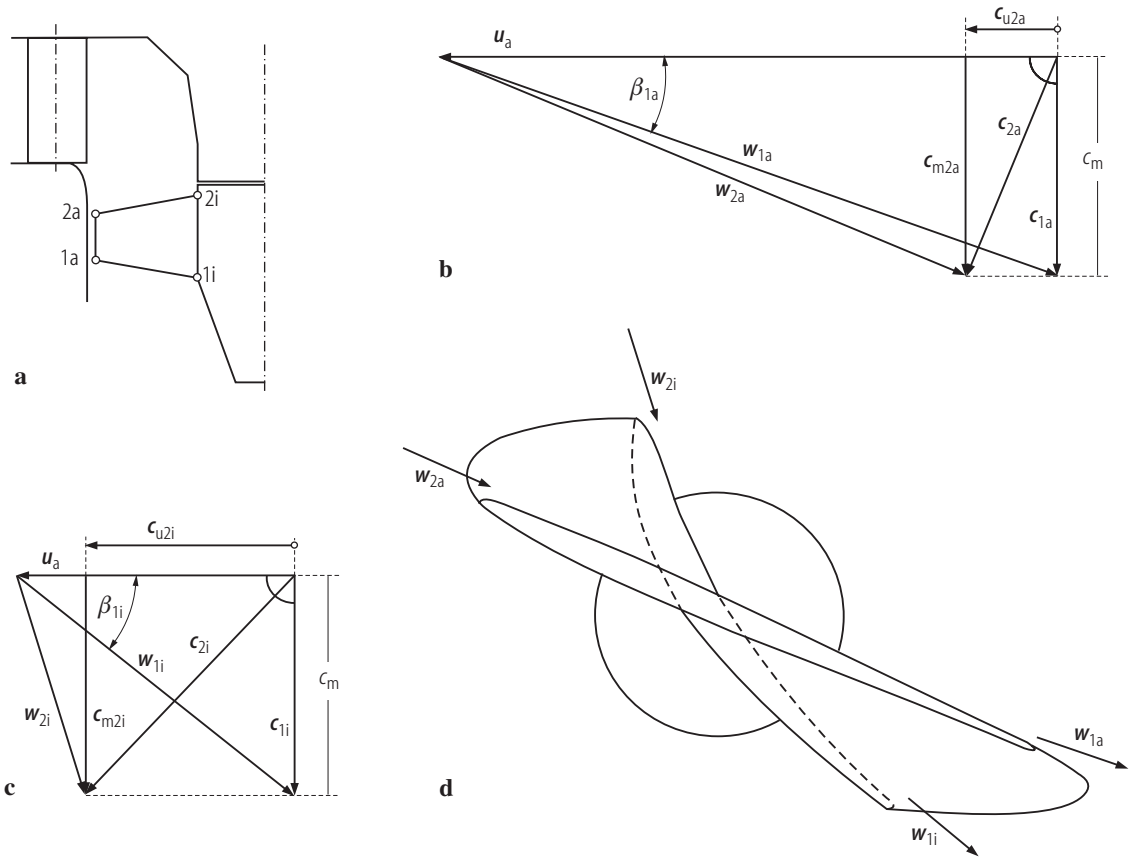

Fig. 2.7.14. (a) Meridional section of a Kaplan turbine with runner entrance and exit at both the tip (index a) and the hub (index i) section. **(b)** Velocity triangles of a Kaplan turbine at the tip section (at best efficiency point). **(c)** Velocity triangles of a Kaplan turbine at the hub section (at best efficiency point). **(d)** Relative velocity $\boldsymbol{w}$ and required shape of the blades.

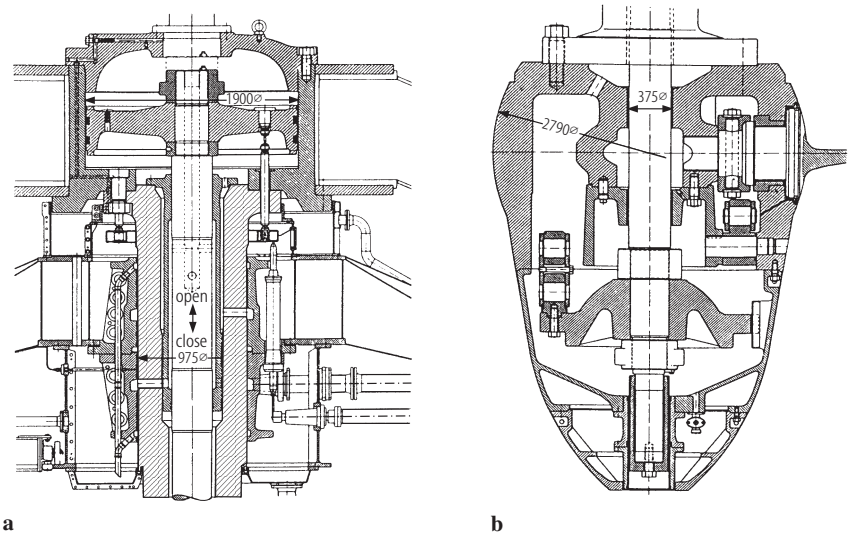

Fig. 2.7.15. Runner blade adjustment. **(a)** Rotating servo motor in generator hub. **(b)** Crosshead in runner hub. [VSH]

2.7.3.2 Hydraulic design of a Kaplan runner

Figure 2.7.16 shows the Kaplan runner of the Aschach power plant. The blades of a Kaplan turbine are always profiled. Their number varies between 3 and 8, dependent on specific speed n_q and head H. The blade number increases with increasing head. To understand this fact, consider the velocity triangles of a Kaplan turbine with a given speed n and a given diameter at different heads. Due to Euler's equation (2.7.3) a higher head results in a greater tangential component c_{u2} at the runner entrance and hence in a stronger deflection of the relative flow within the runner. Consequently, the stronger deflection of the relative flow requires a narrower cascade passage (and therefore more blades) in order to avoid flow separation.

A special design of Kaplan turbines are propeller turbines. They have fixed runner blades which saves the complicated blade adjustment mechanism at the expense of a lower off-design efficiency (see Sect. 2.7.6.2).

As for the spiral case, low-head Kaplan turbines frequently have a semi-spiral instead of a full spiral (see Fig. 2.7.12). Furthermore the semi-spiral is usually fabricated from concrete instead of steel.

2.7.3.3 Manufacture of a Kaplan runner

The profiled blades of a Kaplan runner are usually manufactured from cast steel by milling. The runner material may be a 13% Cr stainless steel, but low-grade cast steel, eventually coated with a welded overlay in critical areas, is also applicable.

2.7.3.4 Operating problems with Kaplan turbines

Due to their high critical cavitation number $\sigma_{T,C}$, Kaplan turbines are frequently subject to cavitation erosion – in addition to "normal" erosion due to abrasive water. Endangered zones are the tip region of the runner blades and the discharge ring. Therefore a periodic repair welding of blades and discharge ring is common practice.

Fig. 2.7.16. Kaplan runner with a diameter of 8.4 m and 5 blades (Aschach, Austria, P_{max} = 75 MW) [VSH].

2.7.3.5 Comparison between Kaplan turbines and Francis turbines

In a certain range of heads there may be a choice between Kaplan turbines and Francis turbines. Indeed, before the development of the Kaplan turbine the Francis turbine was frequently applied to low heads, too. In this case, due to the low specific speed of a Francis turbine, which means low shaft speed as well as low flow rate, usually a step-up gear was necessary for electricity generation. Also, the low flow rate often resulted in Francis turbine designs with several runners per shaft. Generally, the Kaplan turbine offers the following advantages:

- High specific speed, yielding a comparatively high shaft speed;
- High efficiency level over a wide discharge and head range, depending on runner blade adjustment (see Sect. 2.7.6.2).

The disadvantage of the Kaplan turbine, however, is its higher critical cavitation number, resulting in a low, at larger heads frequently negative, suction head. This means a high expenditure for excavation when erecting the power house. Anyhow, the specific investment costs of a Kaplan turbine exceed those of a Francis turbine (see Sect. 2.7.7).

2.7.3.6 Tubular turbines

In a conventional Kaplan turbine (Fig. 2.7.12 and Fig. 2.7.13) the fluid has to pass several bends which cause additional flow losses. As early as 1919 (Patent of Leroy Harza), the idea of a tubular arrangement existed, avoiding unnecessary bends and leading to more favorable flow conditions. The tubular Kaplan turbine is preferably applied to smaller capacities. The maximum output presently realized is 53 MW (Rock Island, USA).

2.7.3.6.1 Example and working principle of a tubular turbine

As an example for a tubular turbine, Figure 2.7.17 shows a section of the Altenwörth power plant (Austria), and Fig. 2.7.18 shows a section of one turbine with the following main data:

- Head: 13,6 m;
- Flow rate: 335 m³/s;
- Speed: 103.4 rpm;
- Shaft power: 41 MW.

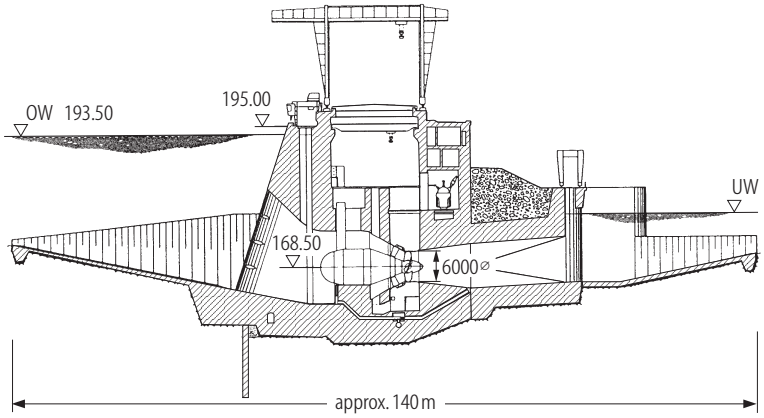

Fig. 2.7.17. Section of the Altenwörth power plant (Austria) [VSH].

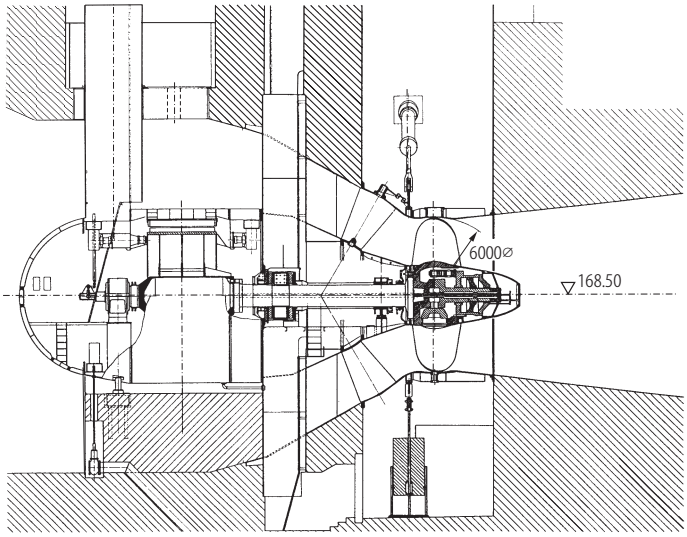

Fig. 2.7.18. Section of the tubular turbine of the Altenwörth power plant (Austria) [VSH].

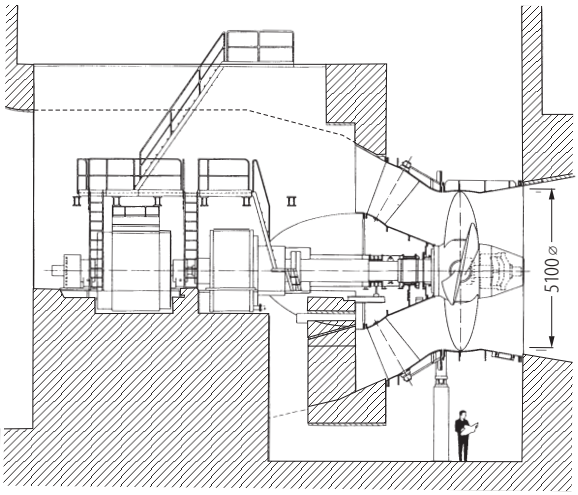

Fig. 2.7.19. Pit turbine (West Enfield, USA, H = 6.4 m, P_S = 11.7 MW) [VSH].

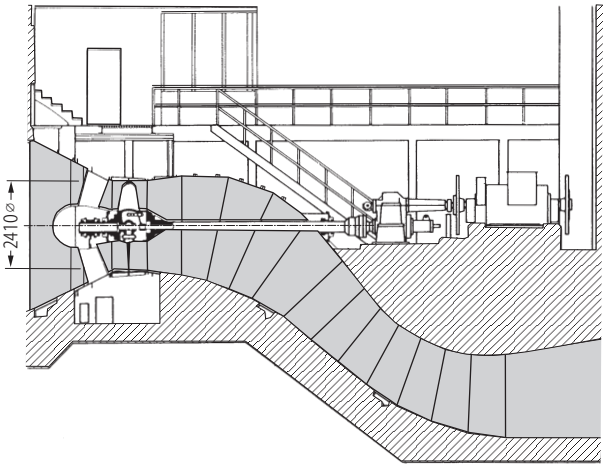

Fig. 2.7.20. S-turbine in Ludwigswehr, Germany with H = 4.5 m and P_S = 0.78 MW [VSH].

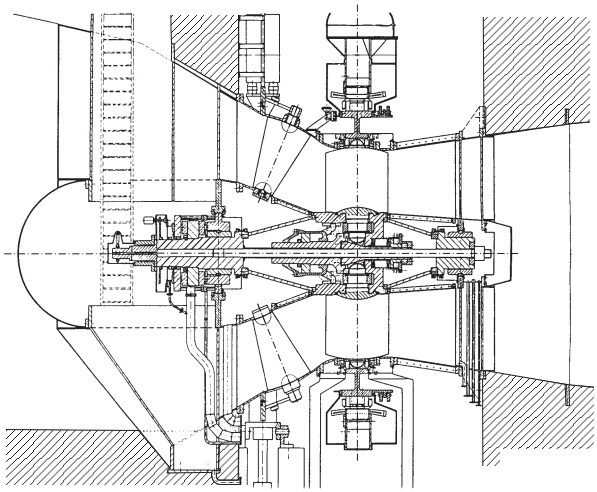

Fig. 2.7.21. Tubular turbine with rim-mounted generator rotor (Weinzödl, Austria, H = 10.3 m, P_S = 8.35 MW) [VAT].

The angular momentum necessary at the Kaplan runner entrance is generated merely by the adjustable guide vanes, the axes of which are arranged on a conical surface. Within the runner the angular momentum of the fluid is decreased in the same manner as in a conventional Kaplan runner. Leaving the runner, the fluid enters the draft tube (diffuser) which, contrary to a conventional Kaplan turbine, is straight. Obviously the total flow path form headwater to tailrace is nearly straight, resulting in a somewhat better efficiency of the tubular Kaplan turbine. The turbine is directly coupled to the generator, as is usual in case of higher capacities.

2.7.3.6.2 Types of tubular turbines

The Altenwörth turbine (Fig. 2.7.17 and Fig. 2.7.18) is a so-called bulb turbine. Beside the bulb turbine, there exists a variety of other designs, especially with regard to small turbines. The most important types of tubular turbines are the

- bulb turbine already mentioned where the generator or an eventual gear are arranged in a bulb;
- pit turbine, where the generator or an eventual gear are arranged in a hollow pier (Fig. 2.7.19);
- S-turbine (Fig. 2.7.20);
- Tubular turbine with rim-mounted generator rotor (Fig. 2.7.21).

2.7.3.7 Comparison between tubular and conventional Kaplan turbines

Compared to conventional Kaplan turbines, tubular turbines offer the following advantages:

- Somewhat better efficiency due to smaller flow losses, avoiding the many bends of a conventional Kaplan turbine;
- Lower excavation expenditures according to the straight, more or less horizontal draft tube.

Disadvantages of the tubular turbines are:

- Considering the bulb or pit turbine, there is limited space for generator, bearings etc. The lack of space requires a more compact mechanical design that is eventually not as durable as that of a conventional Kaplan turbine. Furthermore, the access for maintenance is difficult.
- With many designs, a gear cannot be avoided. This especially applies to smaller turbines.

2.7.4 Pelton turbines

The Pelton turbine, invented by Lester Pelton in 1880, is a tangential jet turbine. It is applied at high heads, presently up to 1869 m (Bieudron, Switzerland). The 3 Bieudron turbines are also the most powerful Pelton turbines today, with a maximum output of 420 MW each.

2.7.4.1 Example and working principle of a Pelton turbine

Figure 2.7.22 shows a section of a turbine of the Naturns power plant (Italy) with the following main data:

- Head: 1129 m;
- Flow rate: 6.18 m^3/s;
- Speed: 500 rpm;
- Shaft power: 61 MW.

The working principle of a Pelton turbine is somewhat different from that of a Francis or Kaplan turbine. Usually atmospheric pressure prevails inside a Pelton turbine. First, the fluid, entering the turbine via a penstock, is accelerated in an adjustable circular nozzle. Then, the jet discharging from the nozzle tangentially impinges a bucket wheel. Due to the tangential position of the jet, the fluid entering a bucket automatically exhibits an angular momentum with respect to the turbine axis. The bucket causes the fluid to deflect by nearly 180°, thus decreasing its angular momentum to zero when operating with design speed. To understand this, consider the velocity diagram in Fig. 2.7.23.

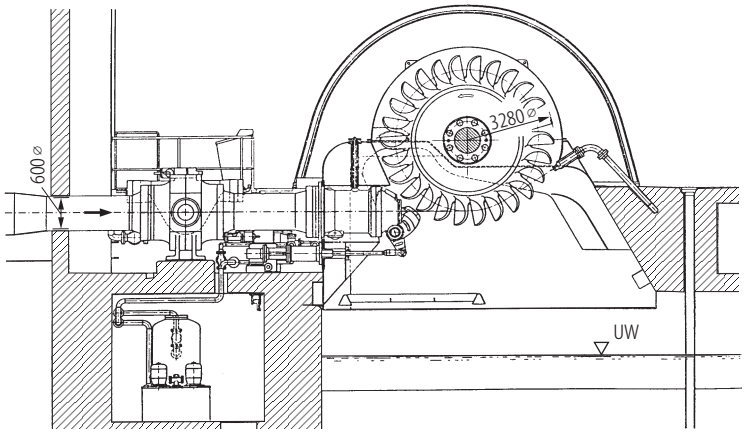

Fig. 2.7.22. Section of a Pelton turbine (Naturns, Italy) [VSH].

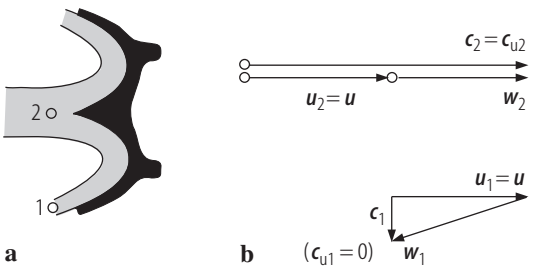

Fig. 2.7.23. (a) Geometry of the bucket with bucket entrance (point 2) and bucket exit (point 1). **(b)** Velocity diagram of a Pelton turbine at design speed.

At the bucket entrance (point 2, radius $r_2 = r$, bucket velocity vector $\boldsymbol{u_2} = \boldsymbol{u}$) the absolute velocity vector $\boldsymbol{c_2}$ is the jet velocity vector. Its tangential component $\boldsymbol{c_{u2}}$ is equal to $\boldsymbol{c_2}$. Hence $r \cdot c_2$ is the angular momentum per unit mass with respect to the turbine axis. The relative velocity vector $\boldsymbol{w_2}$ (viewed from the rotating runner) is equal to the vector difference $\boldsymbol{c_2} - \boldsymbol{u_2}$. Obviously its direction is tangential, too. The bucket causes the relative flow to change its direction by nearly 180°. From a simplified energy balance within the rotating frame of reference we can conclude that the norm of the relative velocity vector is the same at bucket entrance and exit. Thus at the bucket exit (point 1, radius $r_1 = r$, bucket velocity vector $\boldsymbol{u_1} = \boldsymbol{u}$) the relative velocity vector $\boldsymbol{w_1}$ is known (direction according to bucket geometry, norm equal to norm of $\boldsymbol{w_2}$). The absolute velocity vector $\boldsymbol{c_1}$ is equal to the vector sum $\boldsymbol{w_1} + \boldsymbol{u_1}$. $\boldsymbol{c_1}$ has a tangential component $\boldsymbol{c_{u1}}$ which is zero at design speed.

For energetic considerations the Pelton turbine is assumed as a system bounded by a pressure flange upstream the nozzle (point II) and by the bucket exit (point I = 1). As the absolute exit velocity $\boldsymbol{c_1}$ is very small at design conditions, it is usually neglected, and the head H of a Pelton turbine (configuration as in Fig. 2.7.22) is defined as

$$H = \frac{p_{\mathrm{II}} - p_{\mathrm{I}}}{\rho g} + \frac{c_{\mathrm{II}}^2}{2g} + (z_{\mathrm{II}} - z_{\mathrm{I}}) \,. \tag{2.7.13}$$

Assuming an inviscid, incompressible fluid and considering the constant pressure within the turbine, the energy balance between pressure flange (point II) and bucket entrance yields the following equation for the velocity of the jet impinging the bucket:

$$c_2 = \sqrt{2gH} \,. \tag{2.7.14}$$

A simplified energy consideration based on Euler's equation (2.7.3) further yields the optimum bucket velocity u_{opt} for best efficiency (design point):

$$u_{\mathrm{opt}} = \frac{c_2}{2} \,. \tag{2.7.15}$$

The flow rate of the turbine (and hence the output) is controlled by the adjustable nozzle. Usually the nozzle is provided with a needle, actuated by a hydraulic servo motor (Fig. 2.7.24). A jet deflector acts as an additional flow control device, enabling a quick relief of the turbine runner without a quick shutoff of the flow, thus avoiding a detrimental pressure rise in consequence of water hammer surges.

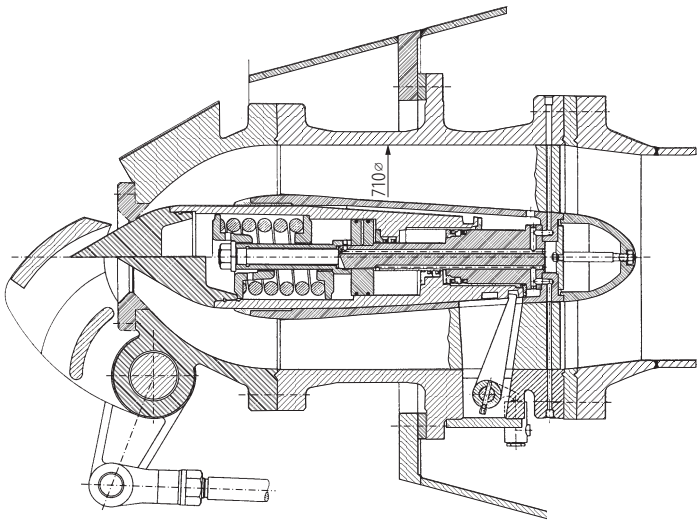

Fig. 2.7.24. Nozzle with needle and jet deflector [VSH].

2.7.4.2 Hydraulic design of a Pelton runner

Figure 2.7.25 shows a large Pelton runner with its typical bucket design. The flow rate of a Pelton turbine is limited by geometrical constraints: The jet diameter usually only amounts to a small fraction of the runner diameter (1/17-1/8, depending on specific speed n_q and head H). The flow rate may be increased by adding nozzles or adding runners: Common designs exhibit up to 6 nozzles per runner and up to 2 runners on one shaft.

The number of buckets is determined by the condition that each fluid particle must be deflected by a bucket instead of passing the runner without being disturbed. A characteristic feature of the bucket is the bucket cutout, carefully designed to minimize flow disturbances when the bucket immerges into the jet.

2.7.4.3 Manufacture of a Pelton runner

Large Pelton runners are usually integrally cast of 13% Cr stainless steel. The final contour of bucket surfaces and bucket cutout is obtained by milling.

2.7.4.4 Peculiarities and operating problems of Pelton turbines

A peculiarity of the Pelton turbine is that due to the constant pressure within the turbine it is not subject to comprehensive cavitation (even if pressure gradients within the deflected jet may cause local cavitation erosion of the buckets).

The bucket wheel is subject to a high alternating mechanical stress caused by the frequent load changes from the discontinuous jet impact. More than once the rupture of a Pelton bucket resulted in severe damages. Hence frequent periodic crack-examinations are necessary. The high jet velocity and the strong flow deflection may result in erosion problems at nozzle and buckets.

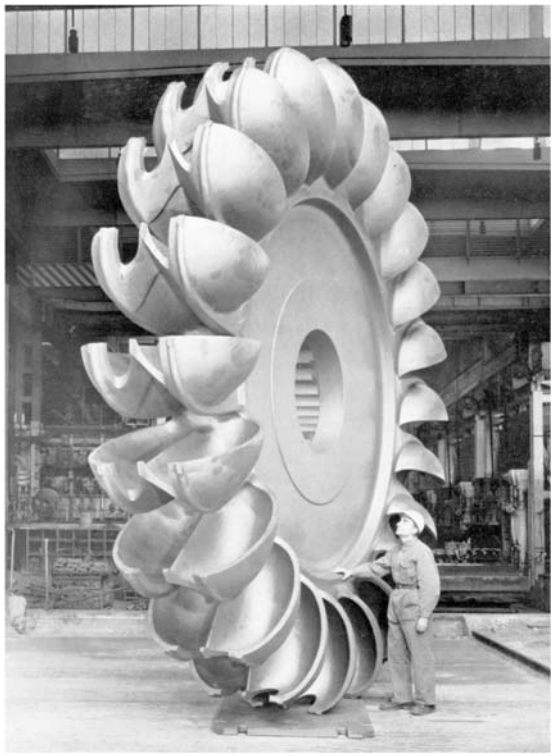

Fig. 2.7.25. Pelton runner, diameter 5.44 m (New Colgate, USA, P_{max} = 166 MW) [VSH].

2.7.4.5 Comparison between Pelton and Francis turbines

In a certain range of heads there may be a choice between Pelton turbines and Francis turbines. The main disadvantage of a Pelton turbine is its low specific speed, which means low shaft speed and low flow rate. The low specific speed usually results in higher expenditures for the electric and mechanical components of a power plant equipped with Pelton turbines as compared to a plant of same discharge equipped with Francis turbines. The Francis turbine is the more sophisticated type of turbine, offering the following advantages:

- Better efficiency at design point than the Pelton turbine;
- Higher shaft speed due to higher specific speed.

However, there are also disadvantages:

- The part load efficiency is lower than that of a Pelton turbine (see Sect. 2.7.6.2).
- To avoid cavitation, high head Francis turbines need negative suction heads which means an arrangement below the tailrace level. In some cases this is not a problem, e.g. if the power house of an upper stage of a series of hydro power plants is arranged beneath the dam of the tail basin. But frequently a negative suction head means expensive excavation.

2.7.5 Michell-Bánki turbines

The Michell-Bánki turbine, based on patents of Michell (1903) and Bánki (1918), is a jet turbine of the cross-flow type. Like the Pelton turbine it is an action turbine (same pressure at runner entrance and exit). But unlike the Pelton turbine, the jet in the Michell-Bánki turbine has a rectangular cross section. Furthermore, the diameter of the cross-flow runner is comparatively small. In consequence, the specific speed of this type of turbine is rather high (n_q = 10-70), enabling the use of this turbine at low heads as well. However, the geometric shape of the cross-flow runner is not suitable for a high output. The Michell-Bánki turbine is therefore merely applied in small hydro power plants. Its maximum output amounts to about 2 MW, its maximum head to about 200 m.

2.7.5.1 Example and working principle of a Michell-Bánki turbine

Figure 2.7.26 shows a section of a Michell-Bánki turbine (Ossberger design). Entering the turbine, the fluid is first accelerated in a converging rectangular channel, thus generating a rectangular jet with a velocity vector $\boldsymbol{c_2}$ at the runner entrance (point 2). A profiled adjustable valve acts as a flow control device, regulating the cross section of the jet. The jet impinges the runner at the entrance (point 2) nearly tangentially. Hence the fluid entering the runner exhibits an angular momentum with respect to the turbine axis due to the tangential velocity component $\boldsymbol{c_{u2}}$ of the jet. Denoting the angle between jet velocity vector $\boldsymbol{c_2}$ and periphery as α_2, the absolute value of the tangential component $\boldsymbol{c_{u2}}$ of the jet velocity vector is

$$c_{u2} = c_2 \cdot \cos\alpha_2 \,. \tag{2.7.16}$$

Crossing the runner, the fluid's angular momentum decreases. At the runner exit (point 1) the water discharges with zero angular momentum when the turbine is operating at design speed. Note that the runner blade row is crossed twice by the fluid jet. A calculation shows that about 80% of the specific blade work is generated at the first passage of the blade row, and only 20% at the second passage.

Downstream the runner a draft tube is provided, mainly in order to raise the tailrace water level up to a position slightly below the runner, thus avoiding a loss of head. Hence the pressure at the turbine runner, usually arranged distinctly above the tailrace level, is less than the atmospheric pressure. The water level within the turbine is controlled by a nose valve.

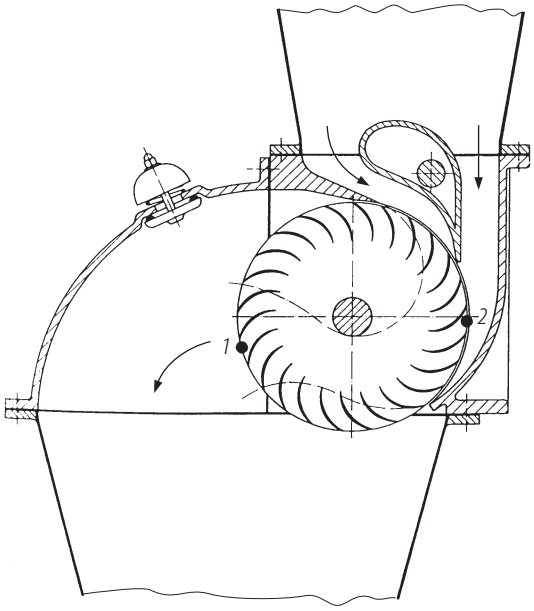

Fig. 2.7.26. Michell-Bánki turbine [OSS].

The hydraulic theory of the Michell-Bánki turbine is similar to that of the Pelton turbine, as both turbines are jet turbines. In close analogy to the Pelton turbine, the optimum blade velocity $u_{2opt} = u_{1opt} = u_{opt}$ of the Michell-Bánki turbine for best efficiency (according to simplified theory) is

$$u_{opt} = \frac{c_{u2}}{2} = \frac{c_2 \cos\alpha_2}{2} . \tag{2.7.17}$$

Like the Pelton turbine, the Michell-Bánki turbine exhibits a constant efficiency level over a wide flow range. This is a characteristic feature of jet turbines. The peak shaft efficiency of a Michell-Bánki turbine amounts to about 80-86%, which is lower than the efficiency of other hydraulic turbines (see Sect. 2.7.6.2). However, the advantage of the Michell-Bánki turbine is its simple construction that allows an easy manufacture.

2.7.6 Performance and control of turbines

2.7.6.1 Basic considerations

Usually a water turbine drives a synchronous generator, which requires a constant speed in order to ensure a constant frequency. Hence the turbine speed has to be kept constant regardless of the flow rate and output of the turbine. This task is accomplished by a speed governor, acting on the flow control device of the turbine (e.g. the adjustable guide vanes of a Francis turbine or the adjustable nozzle of a Pelton turbine).

To understand the performance of a turbine at part load or overload, consider the velocity triangles of a Francis turbine (Fig. 2.7.27). The velocity triangles at best efficiency point were already discussed in Sect. 2.7.1.1 (Fig. 2.7.3). At best efficiency point the relative velocity vector $\boldsymbol{w}_2$ at the runner entrance is parallel to the vanes (shock-less entry), and the absolute velocity vector $\boldsymbol{c}_1$ at the runner exit has no tangential component (zero angular momentum at runner exit). We will now reflect what happens, if the flow rate has to be reduced due to a load reduction. Note that in the velocity triangles the meridional ve-

locity components c_m perpendicular to the tangential direction are proportional to the flow rate. To facilitate the discussion, we will assume that the head, the hydraulic efficiency and of course the speed (and hence the blade velocities) remain constant. Considering the exit triangle, a reduction of the flow rate will result in a reduction of the meridional velocity c_{m1} (= w_{m1}) and hence in a norm reduction of the relative velocity vector $\boldsymbol{w_1}$, the direction of which will remain the same (parallel to the runner blades). Thus the absolute velocity vector $\boldsymbol{c_1}$ (vector sum $\boldsymbol{w_1} + \boldsymbol{u_1}$) will now have a positive tangential component c_{u1} in the direction of rotation. The angular momentum at the runner exit will now be greater than zero, causing a swirl in the draft tube and thus increased flow losses. Furthermore, a positive angular momentum at the runner exit means that according to Euler's equation (2.7.3) the tangential component c_{u2} of the absolute velocity vector at the runner entrance must increase. On the other hand, due to the reduction of the flow rate the meridional velocity component c_{m2} will decrease. Hence the absolute velocity vector $\boldsymbol{c_2}$ will change its direction; the angle α_2 between $\boldsymbol{c_2}$ and tangential direction will decrease. As the direction of $\boldsymbol{c_2}$ is forced from upstream conditions (guide vane position), this means that the guide vanes must close. The relative velocity vector $\boldsymbol{w_2}$ at the runner entrance, resulting from the vector difference $\boldsymbol{c_2} - \boldsymbol{u_2}$, will now have a direction which is not parallel to the runner blades (This fact can be verified by a more detailed calculation). As the fluid can impossibly flow into the blade, a sudden change of the relative flow direction, a so-called inlet shock, will occur, resulting in increased flow losses.

We can now summarize as follows:

- For load reduction, the guide vanes must close;
- At part load, efficiency is reduced by an inlet shock and a draft tube swirl (in the direction of rotation).

A similar discussion about the consequences of a load increase starting from best efficiency point will yield the following statements:

- For load increase, the guide vanes must open;
- At overload, efficiency is reduced by an inlet shock and a draft tube swirl (against the direction of rotation).

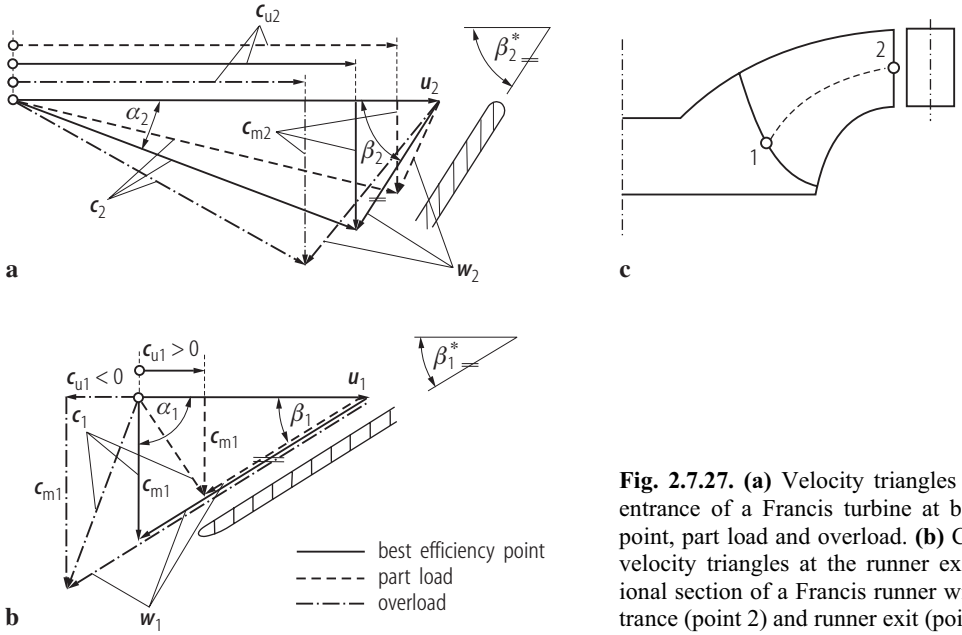

Fig. 2.7.27. (a) Velocity triangles at the runner entrance of a Francis turbine at best efficiency point, part load and overload. **(b)** Corresponding velocity triangles at the runner exit. **(c)** Meridional section of a Francis runner with runner entrance (point 2) and runner exit (point 1).

2.7.6.2 Performance characteristics of turbines

From the above considerations it becomes clear that the efficiency of a Francis turbine will rapidly drop at off-design conditions. The same applies to a propeller turbine with fixed blades. On the other hand, the advantage of the adjustable runner blades of a Kaplan turbine now becomes evident: an appropriate adjustment of these blades minimizes the swirl and inlet losses at off-design conditions. Hence the Kaplan turbine will show a constant efficiency level over a wide range of the flow rate. This is also valid for the Pelton turbine, as the velocity diagram of a Pelton turbine (Fig. 2.7.23) is independent of the flow rate. Figure 2.7.28 shows the efficiency curves of the different types of turbines, confirming our basic considerations. The efficiency also depends on the size of a turbine and on the specific speed. Large hydraulic turbines may eventually reach the following peak shaft efficiencies:

- Francis turbines: $\eta_S = 95\%$;
- Kaplan turbines: $\eta_S = 95\%$;
- Pelton turbines: $\eta_S = 91\%$.

The efficiency of large synchronous generators amounts up to 98%.

In practice, the head of a turbine is not a constant but varies within certain limits. A similar consideration of the velocity triangles as presented above shows that both shock-less entry and zero angular momentum at the runner exit cannot be achieved with another head in case of a Francis turbine. Hence efficiency will drop when operating apart from the rated head. As for the Kaplan turbine, the adjustable blades prove to be beneficial for head variations, too. The performance of a turbine as a function of both flow rate Q and head H is frequently represented by lines of constant shaft efficiency in a Q-H-diagram, also called Hill diagram, as shown in Fig. 2.7.29.

For abnormal operating conditions the performance of a turbine as function of the speed must be known (Fig. 2.7.30).

A characteristic feature of turbines is that the torque decreases with increasing speed. A turbine has its maximum torque at standstill, whereas the torque becomes zero at the so-called runaway speed. It is one of the tasks of the speed governor to prevent the runaway of a turbine. Today water turbines are usually controlled by digital electronic speed governors, the electric signals of which are transformed to the hydraulic actuating system e.g. by means of proportional valves.

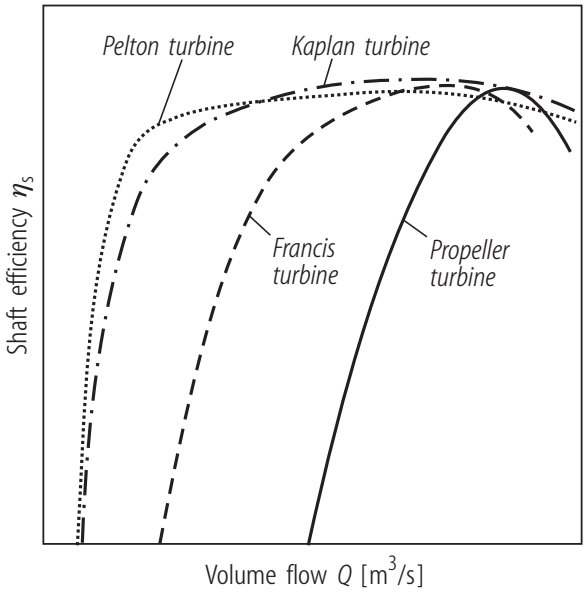

Fig. 2.7.28. Shaft efficiency η_S vs. volume flow rate Q for different types of turbines (at constant head and constant speed).

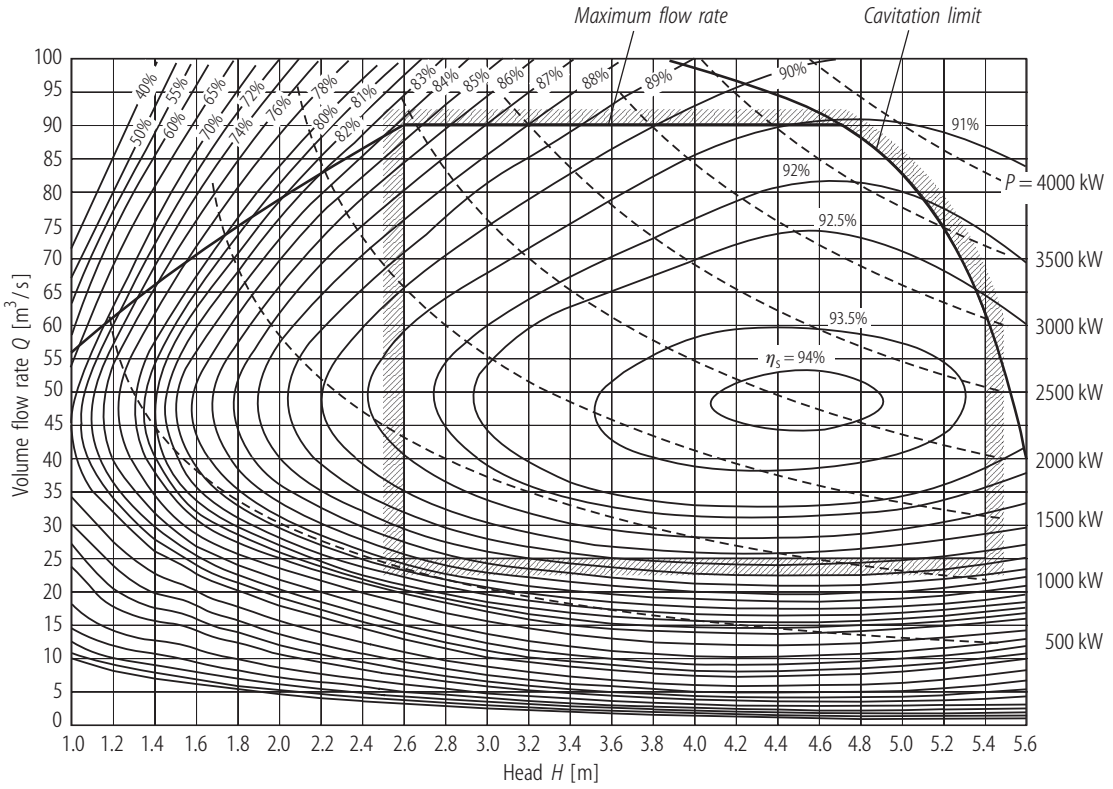

Fig. 2.7.29. Hill diagram of a tubular turbine (curves of constant shaft efficiency η_S in a Q-H-diagram) [EON].

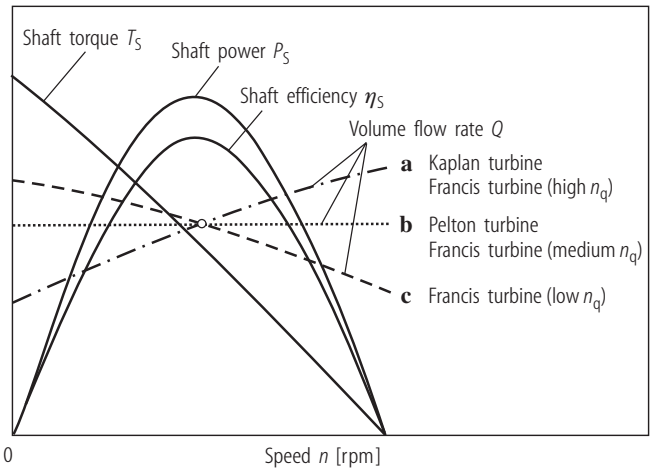

Fig. 2.7.30. Turbine operating data vs. speed n (at constant head and constant position of flow control devices).

2.7.7 Costs of turbines

Table 2.7.1 illustrates typical investment costs (in US$ per kWh) for the different types of turbines, dependent on the capacity (in MW). The lower figures are valid for higher heads, the higher figures for lower heads. In Table 2.7.2, typical investment costs for synchronous generators are presented. Note that the main criterion of the generator investment costs – beside the apparent power – is the number of poles. Hence Table 2.7.2 shows the generator costs (in US$ per kVA) dependent on the apparent power (in MVA) per pole. The number of poles p is a function of grid frequency ν (in Hz) and shaft speed n:

$$p = 120\frac{\nu}{n}. \tag{2.7.18}$$

Apparent power P_a (in MVA) and effective electric power P_{el} (in MW) are related by

$$P_{el} = P_a \cos\varphi, \tag{2.7.19}$$

where $\cos\varphi$ is the power factor the rated value of which is frequently about 0.8.

Table 2.7.1 indicates a strong increase of specific turbine costs with lower capacity. Hence for the economic feasibility of small hydro power plants, simpler turbine designs such as the Michell-Bánki turbine are favorable. The investment costs of a Michell-Bánki turbine (including gear and generator) with a capacity of 200-800 kW ranges from about 550 US$/kW at higher heads to about 1000 US$/kW at lower heads (price basis 2003).

The investment costs presented in this chapter only signify mean, estimated values. Estimation is based on previous publication [89EPR] and actual information obtained by manufacturers. As each hydro power plant is an individual construction, deviations of the cited costs are quite possible.

Generally spoken, the investment costs of turbines plus generators typically amount to only about 20 to 30% of the total investment costs of a hydro power plant. Moreover, hydraulic turbines and generators are a very durable kind of machinery. Their span of life may amount up to 70 years ore even more.

Table 2.7.1. Specific investment costs of turbines dependent on capacity (price basis 2003).

Capacity [MW]	Kaplan turbine costs [US$/kW]	Francis turbine costs [US$/kW]	Pelton turbine costs [US$/kW]
5	460 - 730	160 - 270	160 - 200
10	310 - 580	130 - 180	100 - 150
50	180 - 300	60 - 100	65 - 90
100	150 - 250	40 - 80	55 - 70
200	120 - 190	30 - 70	45 - 60

Table 2.7.2. Specific investment costs of synchronous generators dependent on the apparent power per pole (price basis 2003).

Apparent power per pole [MVA/pole]	Generator costs [US$/kVA]
0.05	380 - 610
0.1	300 - 450
0.5	160 - 230
1	120 - 170
5	65 - 85

2.7.8 References for 2.7 and additional literature

63Qua Quantz, L., Meerwarth, K.: Wasserkraftmaschinen, 11. Auflage, Berlin, Göttingen, Heidelberg: Springer-Verlag, 1963.

72Pfl Pfleiderer, C., Petermann, H.: Strömungsmaschinen, 4. Auflage, Berlin, Göttingen, Heidelberg: Springer-Verlag, 1972.

85Raa Raabe, J.: Hydro Power, Düsseldorf: VDI-Verlag, 1985.

89EPR Electric Power Research Institute (EPRI): Hydropower plant modernization guide, Vol. 1: Hydroplant Modernization, Palo Alto, CA, 1989.

89Raa Raabe, J.: Hydraulische Maschinen und Anlagen, 2. Auflage, Düsseldorf: VDI-Verlag, 1989.

97Gie Giesecke. J., Mosonyi. E.: Wasserkraftanlagen, Berlin, Heidelberg, New York: Springer-Verlag, 1997.

97Koe von König, F., Jehle, C.: Bau von Wasserkraftanlagen, 3. Auflage, Heidelberg: C.F. Müller Verlag, 1997.

Drawings and photos were provided by the following companies:

EON EON Wasserkraft GmbH, Landshut.
OSS Ossberger GmbH & Co, Weissenburg.
VAT VA TECH Escher Wyss GmbH, Ravensburg.
VSH Voith Siemens Hydro Power Generation GmbH & Co KG, Heidenheim.